Clarification of the mechanism reducing torque capacity due to differences between the ideal and actual CVT chain path

Kyohei WATANABE* Jumpei HAYAKAWA* Atsushi IKEDA* Kouhei TOYOHARA* Kazuhiro HAYAKAWA*

Summary

A phenomenon occurred where the torque transmission capacity of a CVT chain did not increase linearly with pulley clamping force. It was confirmed by dynamic analyses and experimental measurements that the deviation of the running radius of the chain from the ideal path caused this phenomenon. Path deviation originated from pulley sheave stiffness. This finding now enables prediction of torque capacity and also supports execution of a suitable pulley stiffness design.

1. Introduction

The variator that provides the shifting capability of a continuously variable transmission (CVT) consists of a pulley assembly and a chain as shown in Fig. 1.

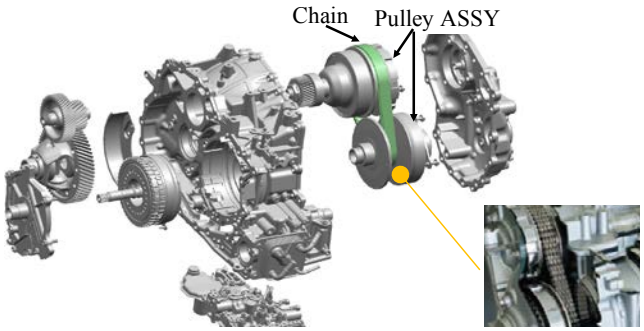

Fig. 1 Structural parts of CVT

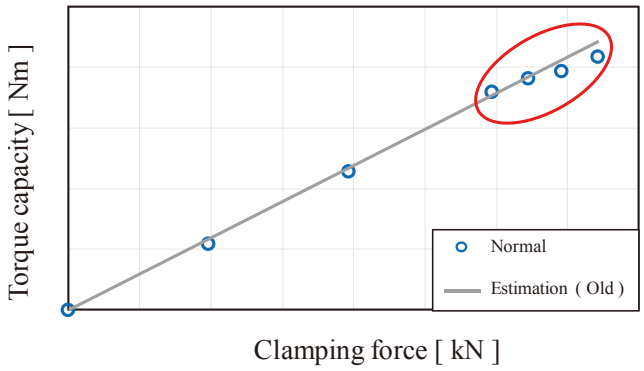

Fig. 2 Torque capacity measurement result

Pulley clamping force is produced by applying hydraulic pressure to the pulley hydraulic chamber. That clamping force generates frictional force between the pulleys and the chain to transmit torque. In general, the torque transmission capacity of a chain is thought to be proportional to pulley clamping force.

During the development of a new variator with high torque capacity, a phenomenon was observed where the torque transmission capacity was not linear relative to pulley clamping force in the region of high pulley clamping force and high torque as shown in Fig. 2. This article presents the results of an investigation undertaken to clarify the mechanism causing this phenomenon, focusing on changes in the running radius of the chain.

2. Investigation of the cause of torque capacity decline

2.1 Calculation equation for torque capacity

Torque capacity due to friction transmission can be expressed as shown in Eq. (1) below.

$$T = F \times R = \Sigma(\mu \times N \times r) \quad (1)$$

T: torque capacity
F: frictional force between chain and pulleys
R: chain average running radius
μ: coefficient of friction of each chain pin
N: clamping force applied to each individual pin
r: running radius of each pin

It was assumed that changes in μ, N and r accompanying an increase in clamping force and torque were the reasons why the torque transmission capacity was not linear

* Hardware System Development Department

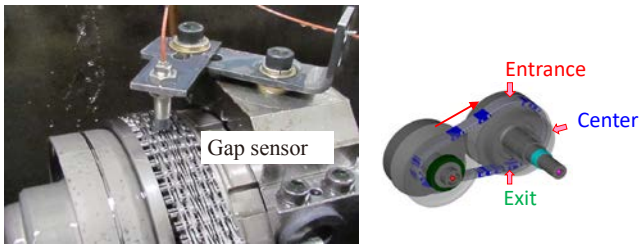

Fig. 3 Gap sensor installation position

relative to pulley clamping force in the region of high pulley clamping force and torque. The amount of change confirmed in each of these parameters is described in the following subsections beginning from 2.2.

2.2 Change in running radius

Changes in the running radius relative to torque were measured under a condition of constant pulley clamping force. As shown in Fig. 3, gap sensors were placed at the entrance, center and exit positions of the chain where it wrapped around the secondary pulley in order to confirm the running radius at each point. The variator test bench shown in Fig. 4 was used to conduct measurement experiments.

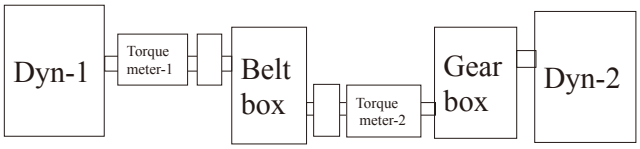

Fig. 4 Variator test bench overview

Table 1 lists the measurement conditions. Figure 5 presents the measured results for the change in the running radius on the secondary pulley in relation to a radius difference of 0 mm when the input torque was 0 Nm. As is also described in Ref. (2), the results show that the running radius of the chain on the entrance side did not change with increasing input torque, but the values at the center and exit on the inside diameter side changed. Figure 6 is a schematic diagram of this radius shift.

As the results in Fig. 5 illustrate, the running radius of the chain changed from the entrance side toward the exit side as input torque increased, which was accompanied by an increase in chain tension on the tension side. As a result, the chain followed a path closer to the inside diameter side at the exit position close to the tension side, which influenced the change in the running radius.

Table 1 Measurement condition

Ratio	-	Low
Input speed	Ni	3,000 rpm
Input torque	T	0→390 Nm
Sec. pulley clamping force	Fs	70 kN

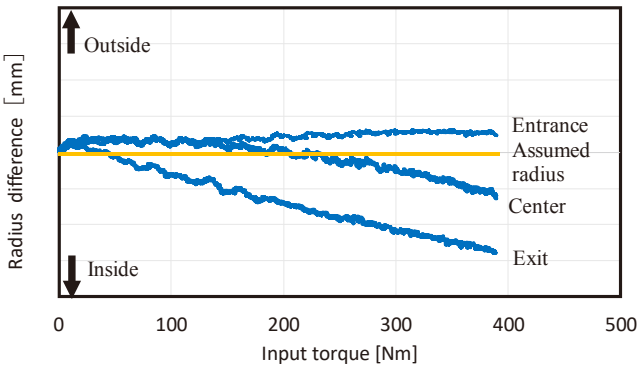

Fig. 5 Radius shift test result

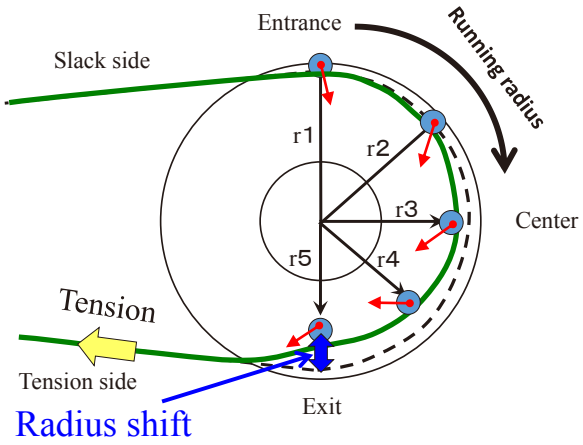

Fig. 6 Radius shift overview

2.3 Change in clamping force applied to each individual pin

Strain gauges were then attached to individual rocker pins in the chain as shown in Fig. 7 to confirm the change in the clamping force applied to each individual pin. The measured strain results from the entrance side to the exit side of the secondary pulley are plotted in Fig. 8 for the measurement conditions listed in Table 2.

The measured strain was proportional to the clamping force of the secondary pulley, and it increased from the entrance side to the exit side where the chain wrapped around the secondary pulley.

The following reason was assumed for the sharp increase in strain toward the exit side as seen in the results in Fig. 8. As described in subsection 2.2, the path traced by the chain near the exit on the tension side was closer to

the inside diameter side. As a result, the pins were further compressed in the section on the inside diameter side, causing the pins themselves to generate large reaction force that increased the amount of strain toward the exit.

With the traditional design method, the running radius between the pins wrapped around the pulley and the sheave face as well as the generated load were treated as being constant values in the design calculations. However, as indicated by the results in Figs. 5 and 8, the running radius between the pins and the sheave face and the generated load constantly change toward the exit owing to the displacement of the pins to the inside diameter side of the pulley. Accordingly, it was reasoned that the running radius r and clamping force N had to be applied to Eq. (1) according to the actual state of each individual pin wrapped around the pulley and thus incorporated into the design calculations.

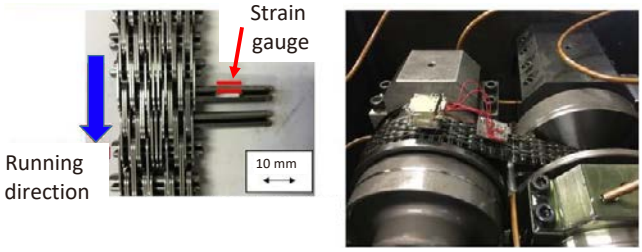

Fig. 7 Locations of strain gauges set on surfaces of pin

Table 2 Measurement condition

Ratio	-	Low
Input speed	Ni	500 rpm
Input torque	T	100 Nm
Sec. pulley clamping force	Fs	30, 50, 70, 80 kN

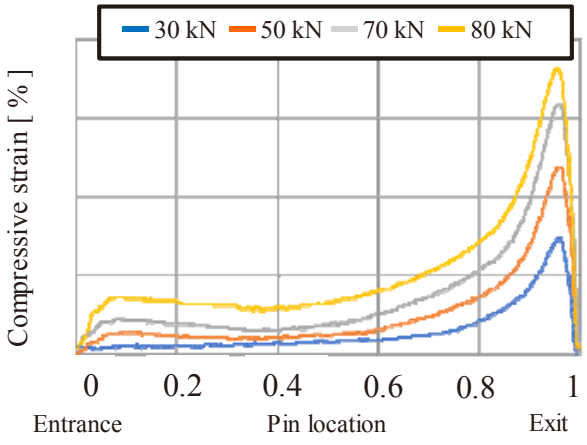

Fig. 8 Measurement of strain gauges set on surfaces of pin

2.4 Estimation of coefficient of friction μ

In general, the coefficient of friction changes according to the sliding velocity and vertical load, and it decreases with increasing oil film thickness h in the boundary lubrication to mixed lubrication regime as indicated by a Stribeck curve.[3] As was made clear in subsection 2.3, the radius between the pulley and the pin end faces changes, so it is assumed that the sliding velocity also varies accompanying such radius changes. In this explication of the mechanism of interest, it was necessary to estimate the coefficient of friction using the sliding velocity and load at the position of each individual pin where the chain wrapped around the pulley. Accordingly, line contact was assumed for the contact between the pulley and the chain; the oil film thickness h under the condition of line contact was calculated using the Dowson-Higgison formula in Eq. (2).

$$\frac{h_{min}}{R}=2.65\left(\frac{\eta_0\bar{u}}{ER}\right)^{0.7}(\alpha E)^{0.54}\left(\frac{W}{ERL}\right)^{-0.13} \quad (2)$$

hmin: minimum oil film thickness
ηo : kinematic viscosity
ū : sliding velocity
E : Young's modulus
A : coefficient of pressure-viscosity
W : load
R : equivalent radius of curvature

Letting the Young's modulus and other parameters in Eq. (2) be constants, it is assumed that the coefficient of friction has a negative first-order correlation with the oil film thickness. Equation (2) can then be replaced by Eqs. (2-1) and (2-2). This assumption was confirmed to be valid on the basis of experimental measurements.

$$\mathrm{hmin} = \mathrm{a}\cdot\bar{u}^{0.7}\cdot W^{-0.13} \quad (2\text{-}1)$$

$$\mu \propto 1/\mathrm{hmin} \quad (2\text{-}2)$$

a: constant

Here, it is necessary to calculate the coefficient of friction μ in relation to the load W and the sliding velocity u. However, because it would be difficult to measure the coefficient of friction for one pin during the operation of the chain, μ was measured in a single part test using a pin-on-disk method as shown in Fig. 9.

Figure 10 presents the coefficient of friction results that were measured when the sliding velocity was varied in a load range of 500-1,600 N/pin. Using the measured results in Fig. 10, the vertical axis in Fig. 11 shows the coefficient of friction μ that was obtained in relation to the calculated product of the sliding velocity and load ($\bar{u}^{0.7}\cdot W^{-0.13}$) on the horizontal axis. The results show that the coefficient of

friction has a negative first-order correlation with the oil film thickness. This indicates that the coefficient of friction μ can be predicted using Eqs. (2-1) and (2-2) that were assumed above.

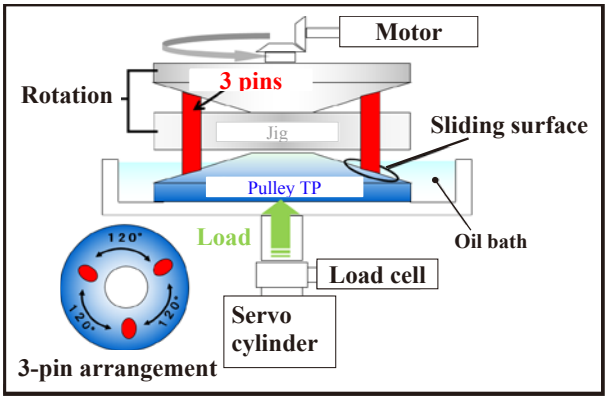

Fig. 9 Pin-on-disk overview

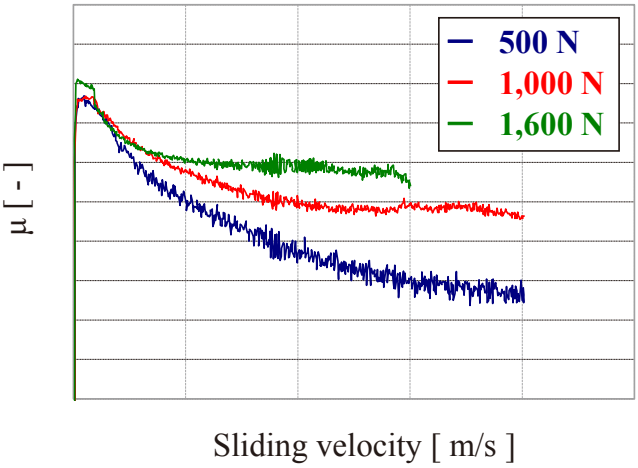

Fig. 10 μ measurement result

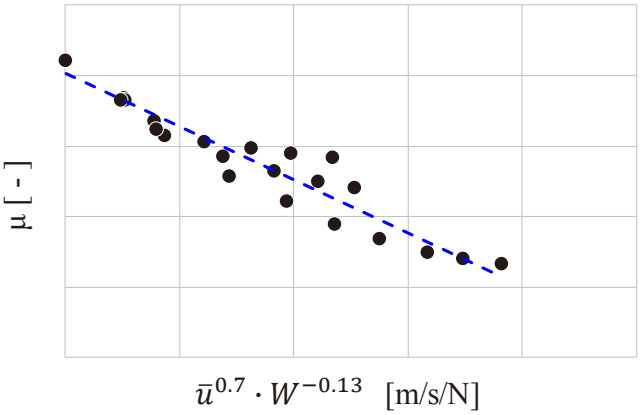

Fig. 11 Friction coefficient result

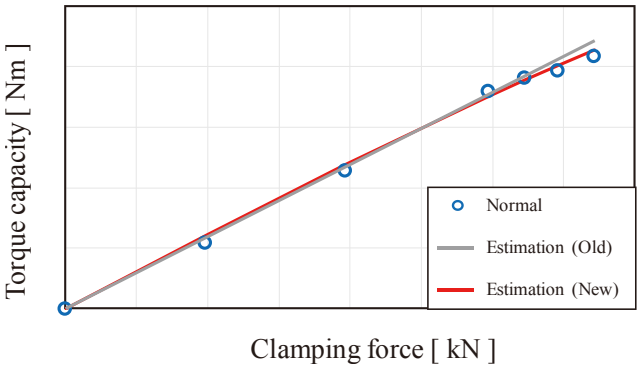

Fig. 12 Comparison of torque capacity between estimation and experimental value

2.5 Torque capacity calculation reflecting the measured results

The measured and calculated μ, N and r values were applied to Eq. (1) to calculate the torque capacity and the results are shown in Fig. 12. As seen in the figure, the values estimated with the new method are closer to the experimental results than those previously estimated.

3. Explanation of mechanism causing non-proportional torque capacity relative to pulley clamping force

3.1 Mechanism causing non-proportional torque capacity

It was shown in section 2 that the torque capacity can be calculated accurately. Therefore, an investigation was made of the mechanism causing the torque transmission capacity to be non-proportional relative to pulley clamping force.

The results in section 2 made it clear that the value of Σr in the torque capacity calculation formula of $\Sigma(\mu \times N \times r)$ in Eq. (1) was smaller than the theoretical calculation.
When Σr becomes smaller, in addition to a decline in torque transmission capacity, the shift toward the inside diameter side becomes larger, thus also increasing the sliding velocity. Because μ has the characteristic that it becomes smaller as the sliding velocity increases, $\Sigma(\mu \times r)$ declines in the region of high pulley clamping force and high torque. This was assumed to be the mechanism causing the torque transmission capacity to become non-proportional.

3.2 Investigation of torque capacity sensitivity to differences in pulley deflection stiffness

It was reasoned that pulley deflection stiffness was the parameter influencing the decline in r and μ. Measurements were made to verify if torque capacity would decline when deflection stiffness was intentionally reduced by shaving

the back side of the pulley, i.e., the portion of the parking lock indicated in the red circle in Fig. 13.

The results presented in Fig. 14 show a tendency for torque capacity to decline further for a pulley with lower deflection stiffness. This indicated that pulley stiffness had to be improved in order to reduce the decline in torque capacity under a high clamping force condition.

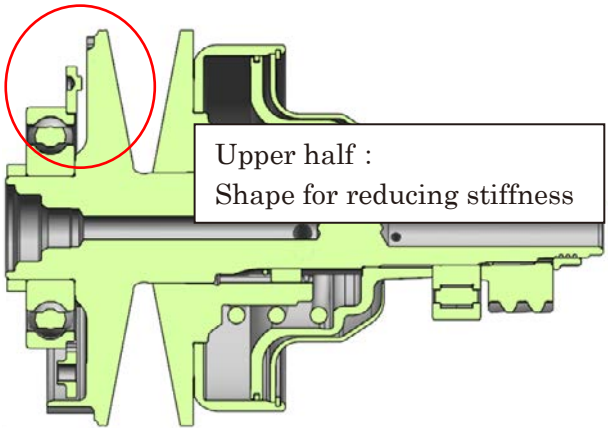

Fig. 13 Overview of pulley stiffness change

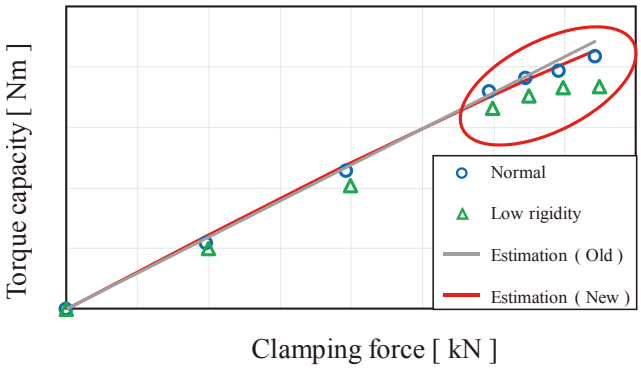

Fig. 14 Torque capacity result between low rigidity pulley and normal pulley

4. Conclusion

- The running radius, clamping force and coefficient of friction of individual chain pins were confirmed on the basis of measured and calculated values. The results were used to calculate the torque capacity, enabling reproduction of the phenomenon where the torque transmission capacity was not proportional to pulley clamping force. The mechanism causing this phenomenon was thus clarified.
- It was found that pulley deflection stiffness must be improved to mitigate reduction of the torque capacity under a high clamping force condition.

5. References

(1) Lubrication Handbook, Yokendo Co., Ltd., p. 265 (1974) (in Japanese).
(2) Nilabh Srivastava, Imtiaz Haque: A review on belt and chain continuously variable transmissions (CVT): Dynamics and control, Mechanism and Machine Theory 44 (2009)
(3) Introduction to Tribology, Yokendo Co., Ltd. (1999) (in Japanese).

Authors


Kyohei WATANABE


Jumpei HAYAKAWA


Atsushi IKEDA


Kouhei TOYOHARA


Kazuhiro HAYAKAWA

Memo